THEORY AND EXPERIMENT FOR THE HEMTs UNDER OPTICAL ILLUMINATION

M.A. Romero, A.L.A. Cunha and A.A.A. de Salles

CETUC, PUC/RJ, Rua Marquês de São Vicente 225, Gávea
CEP 22453, Rio de Janeiro, RJ, Brazil

ABSTRACT

Theoretical and experimental work for the DC and RF performance of depletion mode $Al_{0.3}Ga_{0.7}As$/GaAs HEMTs under optical illumination is presented. Photoconductive effect increasing the 2-DEG channel electron concentration and photovoltaic effect in the gate junction are considered. Optical tuning of a 2 GHz HEMT oscillator and optical control of gain of a 2 to 6 GHz HEMT amplifier are presented and potential applications are described.

INTRODUCTION

The direct optical illumination of microwave semiconductor devices has been an area of growing interest, since various RF control functions such as gain control of amplifiers, oscillator tuning, locking and frequency modulation, as well as switching, mixing, limiting and phase shifting can be achieved [1,2]. Although some authors (e.g. [3-6]) have studied the optical effects in MESFETs, there is a lack of theoretical and experimental work describing the effects of illumination of HEMTs. These are very important microwave devices, since they present extremely low noise performance at frequencies up to several tens of GHz. Also, because they employ heterostructures using III-V semiconductors they are very convenient for use in monolithic integrated circuits (MMICs) or optoelectronic integrated circuits (OEICs).

The major photoeffects arising in the illumination of HEMTs are band-to-band photon absorption in the GaAs and in the AlGaAs layers, generating hole-electron pairs in these regions (Fig. 1). When photons are absorbed only in the GaAs layer, an increase in the electron concentration of the 2-DEG channel occurs (photoconductive effect). When photons are also absorbed in the AlGaAs layer and a high gate bias resistance is present, the photovoltaic effect is dominant [7].

A 2 GHz HEMT oscillator and a 2 to 6 GHz HEMT amplifier were developed on Rogers 6010 substrate (H = 0.635 mm ; ε_r = 10.6) including a high gate-bias resistance ($R_g \cong 1.2$ MΩ) and illuminated with an HeNe laser to investigate the optical control effects. In the experiments a model 155 HeNe Laser from Spectra Physics (λ = 632.8 nm), a FHR01FH AlGaAs/GaAs HEMT from Fujitsu (L = 0.5 μm) without the cover cap and a X25/0.50 microscope objective were used.

PHOTOCONDUCTIVE EFFECT

The photoconductive effect is dominant when the incident photon energy $E_{ph} = h\nu$ is equal to or greater than the GaAs bandgap but smaller than the AlGaAs bandgap. Photoelectrons generated in this layer will experience a vertical field associated with the band bending of the heterojunction and an horizontal field associated with the applied drain-to-surce voltage. Therefore, most of the photoelectrons generated in the GaAs layer will contribute to an increase of the HEMT output conductance and source-to-drain current. An estimation of the electron concentration n_{si} in the 2-DEG channel due to illumination is given by expression (1)

$$n_{si} = \tau_n \cdot \frac{S_{opt}\,\lambda}{h\,c} \cdot (1 - e^{-\alpha_1 d_1}) \qquad (1)$$

where h is Planck's constant, S_{opt} is the incident optical power density, λ is the incident optical wavelength, α_1 is the GaAs optical absorption coefficient, d_1 is the thickness of the GaAs layer, τ_n is the electron lifetime and c is the speed of light in vacuum. Assuming that the variation of the photo-electron concentration n_{si} with the change of the gate bias voltage V_{gs} is negligible, then the drain-to-source photocurrent I_{DSph} can be estimated from expression (2)

$$I_{DSph} = Z \cdot q \cdot n_{si} \cdot v_s \qquad (2)$$

where v_s is the photoelectron drift satured velocity in the 2-DEG channel. Fig. 2 shows a comparison between the estimated and measured photocurrent due to the photoconductive effect in the GaAs

CH2870-4/91/0000-0495$01.00 © 1991 IEEE

layer. An incident optical power (E_{ph} = 1.43 eV) of 0.2 mW focused to $\simeq$ 50µm spot gives an optical power density of $S_{opt} \simeq 10 W/cm^2$ and hence expressions (1) and (2) give $n_{si} \cong 0.8 \times 10^{11}$ electrons/cm^2 and $I_{DSph} \simeq$ 5 mA, respectively, which is in close agreement with the experiments (Fig. 2). The HEMT parameters are given in Table I.

PHOTOVOLTAIC EFFECT

The optical energy absorption in the AlGaAs Schottky gate depletion region produces a photovoltaic effect similar to that experienced in the Schottky gate depletion region of the MESFETs [3]. If a high gate-bias resistance is presented, then a significant photovoltage will be superimposed to the gate-bias voltage applied without illumination. Because the polarity of the photovoltage is the same as forward biasing the gate junction, the drain-to-source current and the gate-to-source capacitance will increase with the increase of the photovoltage developed. The transconductance also changes with illumination. The photogenerated hole concentration Δp is given by

$$\Delta p = \frac{\tau_p}{d_2} \cdot [\frac{S_{opt}\ \lambda}{h\ c}].(1 - e^{-\alpha_2 d_2}) \qquad (3)$$

where τ_p is the minority carrier lifetime, α_2 and d_2 are the absorption coefficient and the thickness of the AlGaAs layer, respectively. Then an estimation of the photovoltage V_{ph} generated in the gate depletion region can be made using expression (4),

$$V_{ph} = \frac{kT}{q} \cdot \ln(\frac{p + \Delta p}{p}) \qquad (4)$$

where k is the Boltzmann's constant and $p = n_i^2/n$ is the equilibrium hole concentration.

Equation (3) is valid only if $\alpha_2.d_2 \ll 1$. If we assume that the hole lifetime τ_p is of the order of 10^{-9}s, we obtain $p = n_i^2/n = 6.25 \times 10^{-12}\ cm^{-3}$. Illuminating the device with an optical power density of $S_{opt} \simeq 10\ W/cm^2$ at E_{ph}= 1.8 eV, expression (3) gives $\Delta p = 4.2 \times 10^{14}\ cm^{-3}$ when d_2= 525 Å. Then using equation (4) we obtain $V_{ph} \cong 1.55V$. In the experiments however, the photovoltage developed is limited to typical values around 0.5-0.7V, when V_{gs} = 0V. This is mainly due to a saturation mechanism, since forward biasing the depletion region reduces its thickness.

Fig.3 shows a comparison between the estimated and the measured photocurrent due to the photovoltaic effect in the gate junction, when the incident optical power density ($E_{ph} < E_{g2}$) is of the order of $S_{opt} \cong 10\ W/cm^2$ (R_g =1.2MΩ). Table II shows a comparison between the applied gate-to-source voltage V_{gs}, the photovoltage V_{ph} and the drain-to-source current I_{ds} when the gate resistance R_g has values of 1.2 MΩ, 100 KΩ and 0Ω.

The total voltage V_{gs_t} measured is given by

$$V_{gst} = V_{gs} - V_{ph} \qquad (5)$$

It can be seen from Table II that a photovoltage V_{ph} = 0.56V is measured when V_{gs}=0V and R_g = 1.2 MΩ.

OPTICAL TUNING

An HEMT oscillator including a gate bias resistance R_g = 1.2 MΩ was optically tuned when the incident optical hower was varied from 0 to 0.5mW. The schematic diagram for the measurements is shown in Fig.4.

Fig.5 shows the optical tuning range measured at different gate to source bias voltage V_{gs}. The output power was around 13 dBm at a dark center frequency of F_o= 1,982 MHz (V_{ds} = 2V and I_{ds} = 10mA). The maximum variation of the output power within the measured optical tuning range was around 0.5dB. It can be seen from Fig. 5 that around 12MHz optical tuning range of the HEMT oscillator was measured. The rate at which the frequency can be changed will be mainly limited by the input circuit RC time constant.

OPTICAL GAIN CONTROL

Fig.6 shows the optical gain control of an HEMT oscillator including a gate bias resistance R_g= 1.2 MΩ, in the frequency range 2.0-6.0 GHz. The HEMT bias were V_{ds}= 3V and V_{gs}= -3V. It can be seen that around 31dB of gain variation was measured at 4.7 GHz when an attenuation of around 18dB without illumination is varied to a gain of around 13dB.

Fig. 7 illustrates the variation of the HEMT amplifier gain for different values of the gate to source voltage V_{gs} at a frequency of 4.6 GHz, when the drain to source voltage V_{ds}= 3V. As the tranconductance does not show a linear performance with respect to V_{gs}, the gain without illumination can be higher than the gain measured under illumination. This is due to the parasitic MESFET operation in the AlGaAs layer of the HEMT.

DISCUSSION AND CONCLUSIONS

The photoconductive and photovoltaic effects in HEMTs were estimated and measured. It has been shown that the photovoltaic effect is dominant when a high gate bias resistance is present.

Optical tuning of a 2 GHz HEMT oscillator was demonstrated, showing around 12 MHz of optical tuning range at an output power of 13 ± 0.5 dB. As much as 31 dB of optical gain control of an HEMT amplifier operating in the 2-6 GHz range was measured.

A comparison can be made with other experiments where the HEMT was illuminated with photon energy smaller than the AlGaAs bandgap [6], when only the photoconductive effect is present. The illumination of the HEMT with photon energy of the order of the AlGaAs bandgap, showing therefore the photovoltaic effect, provides a more efficient control of the HEMT parameters (such as the gate-to-source capacitance and the transconductance), then providing a larger control of the HEMT oscillator frequency and amplifier gain.

These techniques can find important applications in phased array radars and in Optoelectronic Integrated Circuits (OEICs).

ACKNOWLEDGMENTS

The authors are grateful to Prof. M.M. Mosso for his assistance in the experiments. This work was supported in part by TELEBRÁS under contract PUC-TELEBRÁS number 293-88 and by CNPq-Brazilian Research Council.

REFERENCES

[1] Seeds, A.J. and Salles, A.A., "Optical Control of Microwave Semiconductor Devices", IEEE Trans. on MTT, vol. 38, no. 5, May 1990, pp. 577-585.

[2] Hunsperger, R.G., "Optical Control of Microwave Devices", in Integrated Optical Circuit Engineering II (SPIE, vol. 578), S.Sriram, Ed. Bellingham: SPIE, 1985, pp. 40-45.

[3] Salles, A.A., "Optical Control of GaAs MESFETs", IEEE Trans. on MTT, vol. MTT-31, no. 10, Oct. 1983, pp.812-820.

[4] Graffeuil, J., Rossel, P. and Martinot, H., "Light-induced effects in GaAs FETs", Electronics Letters, vol. 15, 1979, pp. 439-441.

[5] R.N. Simons and K.B. Bhasin, "Analysis of Optically Controlled Microwave Millimeter-wave Devices Structures", IEEE Trans. on Microwave Theory and Techniques, vol. MTT-34, no.12, December 1986, pp. 1346-1355.

[6] R.N. Simons, "Microwave Performance of an Optically Controlled AlGaAs/GaAs High Electron Mobility Transistor and GaAs MESFET", IEEE Trans. on Microwave Theory and Techniques, vol. MTT-35, no.12, December 1987, pp. 1444-1455.

[7] A.A. de Salles, "Optical Effects in HEMTs", Microwave and Optical Technology Letters, vol. 3, no. 10, October 1990, pp. 350-354.

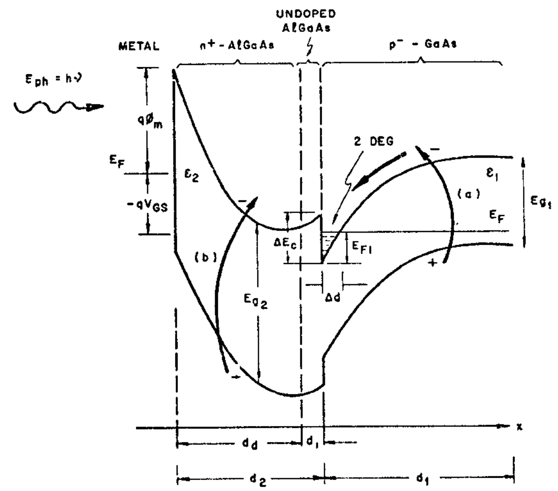

Fig.1 - Hole-electron pairs photoexcited in the AlGaAs and GaAs layers.

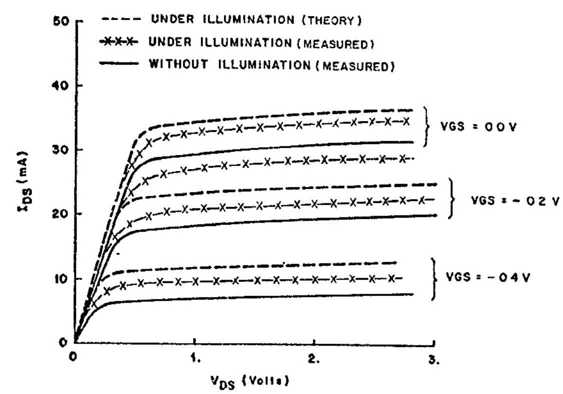

Fig.2 - Estimated and measured I-V characteristics due to photoexcitation of carriers in the GaAs layer (photoconductive effect).

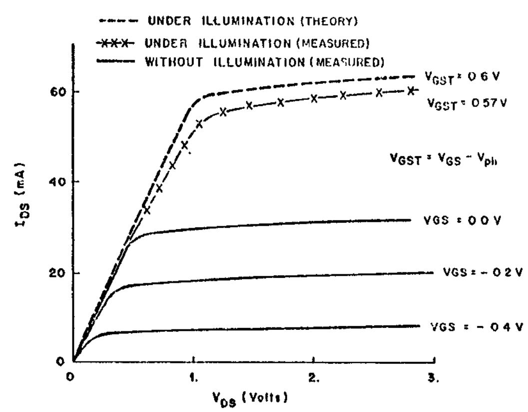

Fig.3 - Estimated and measured I-V characteristics due to photovoltaic effect in the gate junction.

TABLE I. Relevant dimensions and material properties of the HEMT considered in this analysis

Material	Doping density (cm^{-3})	Thickness d	Optical absorption coefficient $\alpha(cm^{-1})$	Bandgap (eV) (T=300 K)	Intrinsic carrier concentration $n_i(cm^{-3})$	Minority carrier lifetime τ (sec)	Relative permitivity ε
1.GaAs	$1x10^{14}$	0.2 microns	$1x10^4$	1.424	$1.79x10^6$	10^{-8}	13.1
2.$Al_{0.3}Ga_{0.7}As$	$1x10^{18}$	525 Angstrons	$1.25x10^4$	1.8	$2.5\ x10^3$	10^{-9}	12.1

z = 200 μm; L = 0.5 μm; Δd = 80 Å; ΔE_c = 0.32 eV; μ = 6800 $cm^2/V.sec$; $v_s = 2 \times 10^7$ cm/s; d_i = 20 Å.

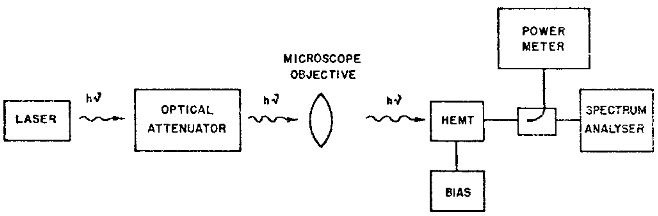

Fig.4 - Schematic diagram for the measurements

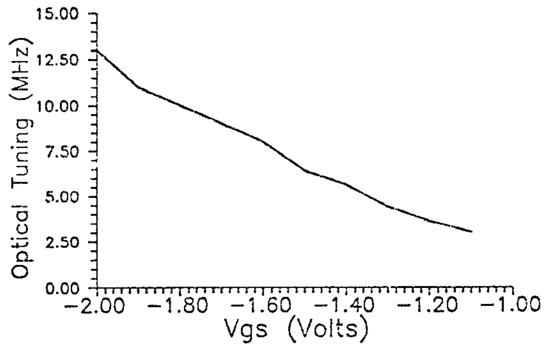

Fig.5 - Measured HEMT oscillator optical tuning range versus gate-to-source voltage V_{gs}.

Table II - Measured photovoltage V_{ph} and drain-to-source current I_{dsi} for different gate bias resistance R_g .

UNDER ILLUMINATION (Rg = 1,2MΩ)			
Vgs(V)	Vgs$_i$(V)	Vph(V)	Ids(mA)
0,017	0,579	0,562	60,0
-0,200	0,561	0,761	59,5
-0,400	0,546	0,946	59,5
-0,600	0,525	1,125	59,0
-0,800	0,477	1,277	58,0
-1,000	0,400	1,400	56,0
-1,200	0,275	1,475	54,0
-1,400	0,138	1,538	51,0
UNDER ILLUMINATION (Rg = 100KΩ)			
0,017	0,139	0,122	51,0
-0,200	-0,069	0,131	45,0
-0,400	-0,247	0,153	37,0
-0,600	-0,420	0,180	29,0
-0,800	-0,575	0,225	20,5
-1,000	-0,715	0,285	14,5
-1,200	-0,826	0,374	9,5
-1,400	-0,917	0,493	7,0
UNDER ILLUMINATION (Pg = 0Ω)			DARK (Rg=0Ω)
0,017	0,017	47,5	46,5
-0,200	-0,198	30,5	38,0
-0,400	-0,395	29,5	28,5
-0,600	-0,598	19,0	18,0
-0,800	-0,792	10,5	8,5
-1,000	-0,992	4,5	3,0
-1,200	-1,119	1,0	0,0
-1,400	-1,390	0,0	0,0

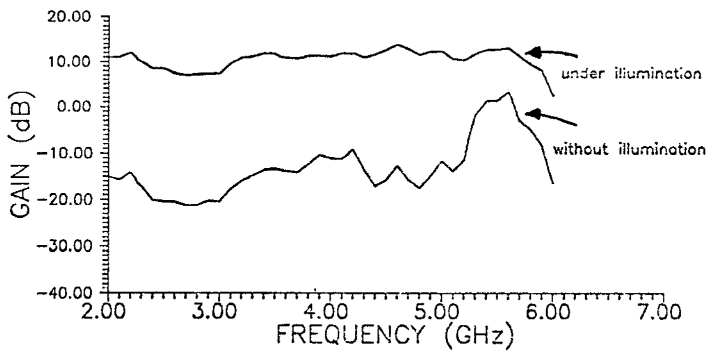

Fig.6 - Measured optical gain control of HEMT amplifier.

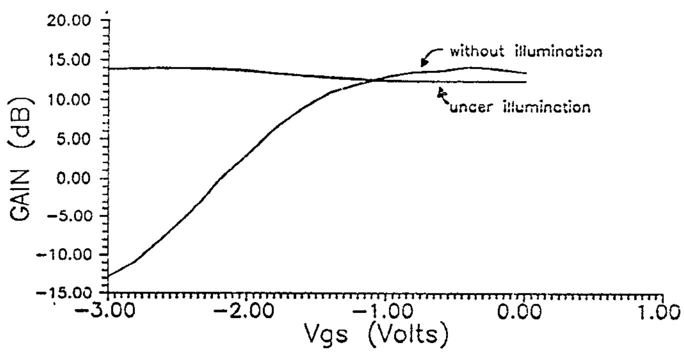

Fig.7 - Measured optical gain variation of HEMT amplifier versus gate-to-source voltage V_{gs}.